Photonic Crystal Waveguide Analysis Using Interface Boundary Conditions

Emanuel Istrate, *Student Member, IEEE,* and Edward H. Sargent, *Senior Member, IEEE*

***Abstract*—Devices based on combinations of photonic bandgap materials are understood intuitively in terms of the dispersion relations of the constituent periodic and locally homogeneous media. Quantitatively, though, photonic crystal-based devices are analyzed using numerical simulations which take no advantage of the *a priori* understanding of underlying periodic building-block materials. Here we unite the quantitative and qualitative pictures of photonic crystal devices and their design. We describe photonic crystals as effective media and impose boundary conditions between photonic crystals and homogeneous materials. We express optical field profiles as superpositions of plane waves in the homogeneous parts and propagating or decaying Bloch modes in the crystals, connected by transmission, reflection, and diffraction coefficients at the interfaces. We calculate waveguide modes, coupling lengths in directional couplers, and coupling between waveguides and point defects, achieving agreements of approximately 1% in frequencies and around 2% in quality factors. We use the new approach to optimize waveguide properties in a forward-going method, instead of the usual iterative optimizations.**

***Index Terms*—Cavity resonators, electromagnetic scattering by periodic structures, interface phenomena, optical directional couplers, optical propagation in nonhomogeneous media, optical waveguide theory, periodic structures.**

I. Introduction

PHOTONIC crystal waveguides are considered one of the main applications of two-dimensional (2-D) photonic crystals. They have received significant attention, both experimentally and theoretically. Since the properties of interfaces between photonic crystals and homogeneous materials are not yet well understood, most methods to analyze the waveguides have used fully numerical methods which produce little generalizable insight into their behavior. Finite-difference time-domain (FDTD) methods [1] predominate. Their use in design forces the use of iterative optimization instead of direct forward design. Other ways of understanding light in photonic crystals, such as through bandstructures [2], are not applicable to devices that are not infinitely periodic.

Optical field profiles within homogeneous dielectrics are customarily and conveniently expressed in a very natural way: propagation is described in a superposition of plane waves which are scattered into one another at the interfaces, as enforced using standard boundary conditions. A similar approach is used in understanding meta-materials [3] in which light is described in terms of plane waves refracted at the boundaries. Propagation through finite-length gratings [4] and the direction of propagation in superprism setups [5] have been analyzed using effective parameters derived from the band structure. We have calculated the boundary conditions at interfaces between photonic crystals and homogeneous materials. These provide complex reflection, transmission, and diffraction coefficients at photonic crystal interfaces and allow us to understand photonic crystal devices in terms of propagating or decaying Bloch modes in the crystals and plane waves in the homogeneous media, all connected by the boundary conditions.

Here we explore the use of the effective medium boundary conditions in the understanding of photonic crystal waveguides and related devices such as directional couplers. We show that the use of boundary conditions allows us to analyze quantitatively the behavior of the devices in the same way in which we have intuitively understood their behavior qualitatively. We also show the flexibility of our method in considering a range of structures, including situations where not all of the interfaces are parallel.

When light is incident from a homogeneous material onto a photonic crystal, some will be reflected, with a given amplitude and phase, some may be diffracted back into the homogeneous material, again with given amplitudes and phases, and some may be transmitted, if the crystal allows it, by exciting one or more propagating Bloch modes of the crystal. Using the boundary conditions, we can determine these reflection, diffraction, and transmission coefficients at photonic crystal interfaces. They are obtained by matching the photonic crystal Bloch modes to the plane waves of the homogeneous material, as described in the Appendix. Complex Bloch modes [6], [7] are used if light is incident on a photonic crystal in its stopband. In that case, the reflection and diffraction coefficients become complex, similar to the complex Fresnel coefficients for light past the critical angle at dielectric interfaces.

Using the reflection and diffraction coefficients allows one to calculate the resonant mode frequencies in photonic crystal waveguides in a simple and natural way. Light in the waveguide core will have a transverse wavevector component, perpendicular to the interfaces. The phase change induced by this wavevector across the core plus the phase change obtained from the complex reflection coefficients at the interfaces must produce constructive interference in order for the mode to exist. This is a very simple condition to enforce. The reflection coefficients can be calculated once for a given photonic crystal geometry and stored in a table. The remaining computations are very fast, as will be shown below.

Manuscript received July 12, 2004; revised September 30, 2004. This work was supported by the Natural Sciences and Engineering Research Council (NSERC) and industrial and government partners through the Agile All-Photonic Networks (AAPN) Research Network.

The authors are with the Department of Electrical and Computer Engineering, University of Toronto, Toronto, ON M5S 3G4, Canada.

Digital Object Identifier 10.1109/JQE.2004.841615

In most cases of practical photonic crystal waveguides, the core will have a high refractive index. In this case, the photonic crystal can diffract each incoming plane wave into multiple waves. A resonant mode exists when we obtain a given mixture of plane waves that remains stationary in the guide.

Line and point defects in photonic crystals have been considered before using a plane-wave expansion in a supercell arrangement and with several tight-binding treatments using Wannier-like equations [8], [9]. The advantage of our method lies in the fact that we separate the interface effects from the propagation. Hence, we can change the size of the defects without the need to rerun simulations.

In this paper, we describe in detail the computation of guided modes in photonic crystals, using the complex reflection and diffraction coefficients. We start with a simple example of a waveguide in a square lattice, with a low-index core. Next, we present cases encountered more often in practice: waveguides with high-index cores and triangular photonic crystals. We then study coupling between neighboring waveguides, again using the complex transmission, reflection, and diffraction coefficients. We finish by analyzing the coupling of photonic crystal waveguides to point defects.

II. Guided Mode Conditions

We have reduced the photonic crystal to an effective medium characterized by a complex dispersion relation and complex diffraction coefficients at the interfaces. Here, we note that specular reflection is a special case of diffraction. We can now employ the same treatment as for dielectric waveguides. We expect a guided mode to propagate as a superposition of plane waves in the core and exponentially decaying waves in the claddings. The exponential decay is given by the complex photonic crystal modes in the stopbands, which have an imaginary Bloch vector.

As is the case with all waveguides, the propagation vector along the waveguide must be the same throughout the structure, and it forms the waveguide propagation constant β. We find the modes of the structure by fixing β and searching for allowed frequencies ω as follows.

A. Low-Index Core

We start our analysis with an air core in a square photonic crystal of silicon rods in air. Its analysis is very simple due to the fact that, at frequencies in the first bandgap of the structure, the propagation vectors in the core are smaller than the Brillouin zone of the crystal. As a result, the crystal can only reflect plane waves. Diffraction into other waves is impossible, which allows us to only consider one set of plane waves.

We consider the waveguide geometry shown in Fig. 1. Having chosen a β, the reflection coefficients are computed in the Appendix as a function of frequency. In the bandgap, they have unit magnitude and a phase ϕ_r. The plane waves in the core will have a transverse propagation vector given by

$$k_x = \sqrt{\left(n_c \frac{\omega}{c}\right)^2 - \beta^2} \tag{1}$$

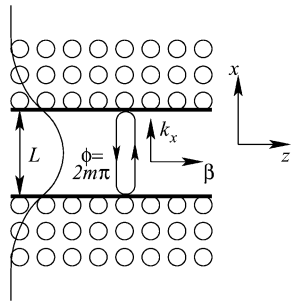

Fig. 1. Structure of a low-index waveguide considered.

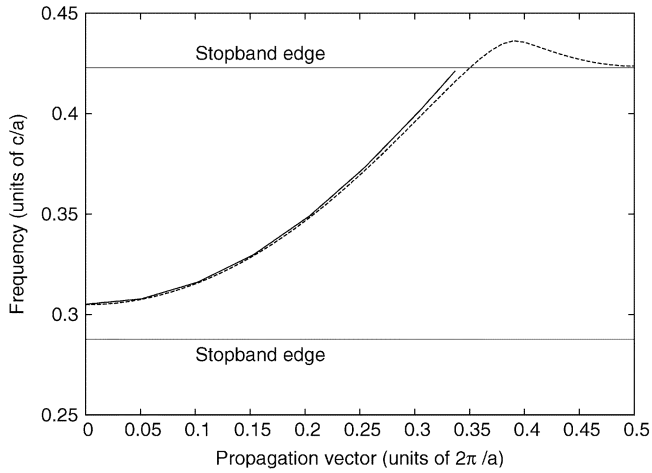

Fig. 2. Dispersion relation of the waveguide from Fig. 1. The solid line represents our work. The dashed line is from MPB simulations.

where n_c is the refractive index of the core. In order to have a resonant mode in the structure, the wave must interfere constructively with itself after a round-trip in the guide. We write this condition as

$$2\phi_r + 2k_x L = 2m\pi \tag{2}$$

where m is an integer.

By repeating the above for a number of values of β, we can map the entire dispersion relation of the waveguide. In Fig. 2, we show the dispersion relation for the structure in Fig. 1 where the radius of the cylinders is $r = 0.2a$. a is the lattice constant of the crystal. The computation was done for the TM polarization, where the electric field is parallel to the rods. The core is obtained by removing a row of rods. We compare our results with simulations using the MIT Photonic Bands (MPB) package [10]. Our results agree very well with the simulations. The small discrepancy at higher values of the propagation vector appears because we neglected the higher order diffraction of the plane wave at the cladding interfaces. For the low-index core, this diffraction produces evanescent waves. However, for larger values of the propagation constant, the evanescent decay length increases and starts playing a more important role. By neglecting this, we effectively assume that the field profile in the core is a plane wave, without any periodicity induced by the neighboring crystals. Higher order diffraction will be included in the next subsection.

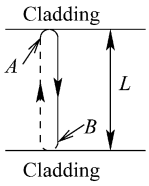

Fig. 3. Setup used to find guided modes. The waves propagate from points A to B and back to A.

B. High-Index Core

We now consider the case encountered more often in practice of a photonic crystal made of a triangular lattice of holes etched in a semiconductor. The core is made of the same semiconductor by removing a row of holes. In this case, much larger propagation vectors are allowed in the core, and the photonic crystal can diffract the plane waves from a propagation vector β to $\beta \pm 2\pi/a$. The guided mode must then contain a superposition of all of the diffracted plane waves. In most cases encountered in practical waveguides, there will be two or three plane waves.

We denote the amplitude and phases of the individual plane waves by the phasors E_i, their propagation constant along the waveguide by β_i, and their transverse wavevector component by k_{xi}. i labels the individual plane waves. Since the diffraction is done by a photonic crystal of lattice constant a, we have $\beta_i - \beta_j = 2\pi m/a$, for integer values of m. Equation (1) still holds. We denote the diffraction coefficients from plane wave i to j by d_{ij}. With this notation, d_{ii} represents specular reflection. d_{ij} will in general not have unit magnitude any more, but the total optical energy must be conserved among the plane waves.

We allow the waves to propagate as shown in Fig. 3, from points A to B. We denote the fields at A by E_i and the fields at B by E_i'. The fields at the two points are related by the following equations:

$$\begin{aligned} E_1' &= (E_1 d_{11} + E_2 d_{21} + E_3 d_{31} + \cdots) e^{ik_{x1}L} \\ E_2' &= (E_1 d_{12} + E_2 d_{22} + E_3 d_{32} + \cdots) e^{ik_{x2}L} \\ E_3' &= (E_1 d_{13} + E_2 d_{23} + E_3 d_{33} + \cdots) e^{ik_{x3}L} \\ &\vdots \end{aligned} \tag{3}$$

This can be written in matrix form as

$$\begin{pmatrix} E_1' \\ E_2' \\ E_3' \\ \vdots \end{pmatrix} = \begin{pmatrix} m_{11} & m_{12} & m_{13} & \cdots \\ m_{21} & m_{22} & m_{23} & \cdots \\ m_{31} & m_{32} & m_{33} & \cdots \\ \vdots & & & \end{pmatrix} \begin{pmatrix} E_1 \\ E_2 \\ E_3 \\ \vdots \end{pmatrix}. \tag{4}$$

We denote the matrix above by $\mathbf{M}$. We obtain a similar matrix $\mathbf{N}$ which completes the round trip, relating the fields at point B to those at A.

As before, we require that the fields after one round trip be equal to the starting fields as follows:

$$\begin{pmatrix} E_1 \\ E_2 \\ E_3 \\ \vdots \end{pmatrix} = \mathbf{NM} \begin{pmatrix} E_1 \\ E_2 \\ E_3 \\ \vdots \end{pmatrix} \tag{5}$$

which can be solved as an eigenvalue equation by requiring that the eigenvalue of $\mathbf{NM}$ be equal to 1. If the crystals on the two sides of the guide are identical, forming a symmetric waveguide, we can work with one half round trip, requiring that the fields at point B be equal to those at A for even modes or the exact negative for odd modes. This means that the eigenvalue of $\mathbf{M}$ must be equal to ± 1.

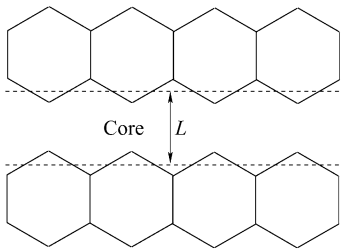

Fig. 4. Interfaces between cladding and core of a waveguide in a triangular lattice. The diffraction coefficients are computed along dashed lines.

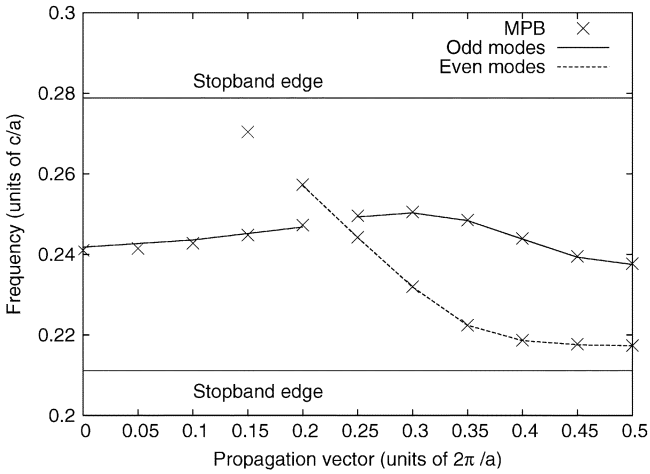

Fig. 5. Dispersion relation of a waveguide in the triangular crystal. The lines are from our computations. Points are from MPB.

We note that the eigenvalues will always have unit magnitude for frequencies in the stopband of the crystal, since the total optical energy is conserved. However, a guided mode only appears when the eigenvalue also becomes real and conserves the phase relationships between the plane waves.

Triangular lattices are used in the same manner as square lattices. However, the unit cells of the cladding photonic crystal are hexagonal, and the interface between the unit cells and the waveguide core does not form a straight line any more, as shown in Fig. 4. The computation of the diffraction coefficients is normally done at the edge of the unit cells. However, since we excite plane waves in the core, it is easier to perform the mode matching along straight lines, such as the dashed lines in Fig. 4, as long as they do not cross any photonic crystal holes.

In Fig. 5 we show the dispersion relation of a waveguide obtained from a triangular photonic crystal of holes in a GaAs–AlGaAs slab waveguide with an effective index of 3.4. The holes have a radius of 0.3 times the lattice constant. The core was obtained by removing a row of holes. We use TE polarization, with the magnetic field parallel to the holes. Again, we compare our results with MPB simulations and obtain very good agreement. The largest discrepancy in the guided mode frequency is 1.1% of the bandgap width, which can be reduced by including even higher orders of diffraction into evanescent waves. For symmetric guides, our method allows us to easily identify even and

odd modes from the sign of the eigenvalue, as described above. There is no need to analyze the mode profiles.

In the case of waveguides with semiconductor cores, most of the time there will be two plane waves, one with β_1 and the other with $\beta_2 = \beta_1 - 2\pi/a$. β_1 is positive and lies in the first Brillouin zone of the crystal, while β_2 is negative. The two plane waves carry power in opposite directions along the waveguide. The direction of power flow in the waveguide will be given by the relative amplitudes of the plane waves. It should be noted that, in the symmetric crystals studied here, we can still have modes carrying power in the opposite direction, with β_1 negative and in the first Brillouin zone and β_2 positive.

C. Waveguide Design

By separating the effects of the photonic crystal from the propagation of plane waves in the waveguide core, the method presented here is well suited to the design of waveguides. One common problem is to find the necessary waveguide width to achieve certain properties, such as a given phase or group velocity. We show below how this problem can be solved for the case of two plane waves in the core of a symmetric guide. In this case, we can rewrite the mode condition from above, requiring that eigenvalues of matrix $\mathbf{M}$ have value ± 1 as follows:

$$e^{i(k_{x1}+k_{x2})L}(d_{12}d_{21} - d_{11}d_{22}) \pm [e^{ik_{x1}L}d_{11} + e^{ik_{x2}L}d_{22}] = 1 \tag{6}$$

$$k_{x1} = \sqrt{\left(\frac{n_c\omega}{c}\right)^2 - \beta^2} \tag{7}$$

$$k_{x2} = \sqrt{\left(\frac{n_c\omega}{c}\right)^2 - \left(\beta - \frac{2\pi}{a}\right)^2}. \tag{8}$$

This forms essentially the dispersion relation for the waveguide. In the above equations, the positive sign is used for even modes and the negative for odd modes. For a given combination of ω and β, giving the desired phase velocity, the required waveguide width L can be found rapidly, since the diffraction coefficients d_{ij} are known.

If a given group velocity is desired, (6) can be differentiated with respect to β, and the resulting equation can again be solved for L. A further differentiation would produce an equation for the group velocity dispersion.

For the dispersion relation shown in Fig. 5, there is only one plane wave allowed for $\beta < 0.1 \times 2\pi/a$. In this case, (6) can be simplified even more to obtain

$$L = \frac{m\pi - \phi_r(\beta,\omega)}{\sqrt{\left(n_c\frac{\omega}{c}\right)^2 - \beta^2}} \tag{9}$$

where ϕ_r is the angle of the reflection coefficient and m is an integer.

III. Waveguide Coupling

A very important device realized using waveguides is the directional coupler, which allows switching of light from one arm to the other or splitting of power between two waveguides.

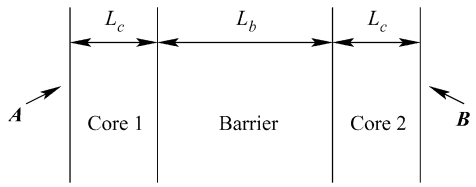

Fig. 6. Two guides forming the directional coupler.

It consists of two waveguides spaced closely enough such that light can couple from one to the other over a characteristic length, called the coupling constant. Until now, coupling between the guides has been computed by running simulations on a cross section of the device, including many unit cells. In this section, we present an analysis of the photonic crystal directional coupler using the boundary conditions described above.

We proceed in a manner similar to the one described in [11] and compute the supermodes of the structure consisting of the two parallel waveguides separated by a thin barrier. The modes appear in pairs, one at a frequency slightly lower and one slightly higher than the mode of the equivalent single-guide structure. One of the modes will have even symmetry and the other will have odd symmetry. The superposition of the two, with a certain phase relationship, will concentrate all of the energy in one guide. At the opposite phase relationship, all of the energy will move to the other guide. The beating between the modes, propagating with slightly different propagation constants, produces an oscillation of energy between the two guides.

A. Transfer Matrix Setup

We use again the interface diffraction coefficients to calculate the supermodes. Since the structure is more complex, with four interfaces, we organize the equations in the Appendix using the transfer matrix method (TMM) [12]. Traditionally, the TMM is used with a single allowed wave in each direction. Here, we use multiple waves, as required by our structures with multiple plane waves and multiple Bloch modes.

The waveguide structure to be solved is shown in Fig. 6. Vectors $\mathbf{V_A}$ and $\mathbf{V_B}$, representing the fields at points A and B, are related by the following matrix product:

$$\mathbf{V_A} = \mathbf{M_{bh}M_{c1}M_{hb}M_bM_{bh}M_{c2}M_{hb}V_B} \tag{10}$$

$$\equiv \mathbf{MV_B} \tag{11}$$

where $\mathbf{M_{c1}}, \mathbf{M_{c1}},$ and $\mathbf{M_b}$ are the propagation matrices for the two cores and the barrier, while the other matrices in (10) describe the interfaces. All matrices are calculated in the Appendix. Guided modes of this structure must not have waves propagating to the right at point A and to the left at B. This means that the determinant of the top-left corner of matrix $\mathbf{M}$ must be zero.

We note that this TMM treatment could also be applied to the simple waveguides considered in the previous section. The results would be equivalent.

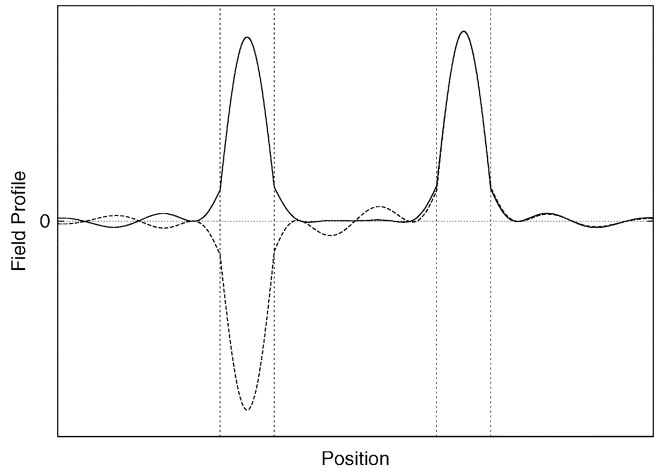

Fig. 7. Profiles of even mode (solid line) and odd mode (dashed line) in the directional coupler. The vertical lines mark the positions of the cores.

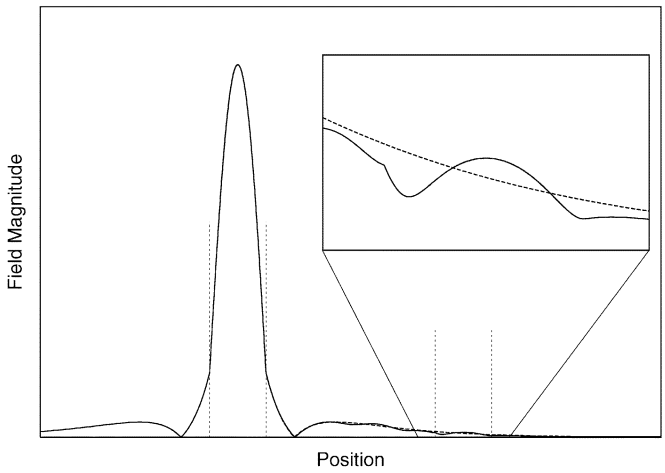

Fig. 8. Superposition of even and odd modes (solid line). Mode of a single guide (dashed line). Inset shows the superposition in the core on the right.

B. Coupling Constants and Power Transfer

Using the TMM and the boundary conditions, we compute the two closely spaced mode propagation constants and profiles of the directional coupler.

As an example, we consider the waveguides from the previous section, using the triangular photonic crystal. The cores are formed by removing a row of holes, and the barrier between the guides is made of three rows of holes. The supermodes of the coupler will be close to those described by the dispersion relation in Fig. 5. We choose to work in the single-mode region of that graph, at a frequency of $0.219c/a$ and a propagation vector near $0.35 \times 2\pi/a$. We obtain for the supermodes of the coupler the propagation vectors $0.3821 \times 2\pi/a$ and $0.3977 \times 2\pi/a$. The mode frequencies agree with full simulations to within better than 0.5% of the stopband. As described in [11], we obtain a beat length between the modes of

$$L_B = \frac{2\pi}{|\beta_1 - \beta_2|} = 64.1a \tag{12}$$

corresponding to a coupling length equal to 32 lattice constants.

In Fig. 7, we show the profiles of the two supermodes. The phase of the modes was chosen such that their imaginary part vanishes in the cores. We show the real part of the modes. In the photonic crystal, we only show the propagating and decaying parts of the Bloch modes. To obtain the true electric field profile, this should be multiplied by the periodic part of the Bloch mode.

When light is launched into one of the two guides, it will excite a superposition of the even and odd modes. Through their beating, these modes will concentrate the light alternatively in each guide. Fig. 8 shows the magnitude of the superposition, when the light is concentrated in the left guide. The dashed line shows the mode profile of the left guide, if there was no guide on the right. We see that the energy in the guide on the right is almost the same as the energy in the tail of the mode from the guide on the left, if there was no guide on the right. This shows that complete power transfer is possible between the guides.

IV. Coupling to Point Defects

The complex reflection coefficients can be used to accurately compute the resonant modes of point defects. In this section, we investigate the coupling between a point defect and a waveguide located nearby [13], as illustrated in Fig. 9. Light will couple from the waveguide to the defect, where it can resonate if it has the right frequency. At resonance, high light intensities will accumulate in the defect and light in the waveguide will be reflected. Away from resonance, the defect will have a very small effect on the waveguide.

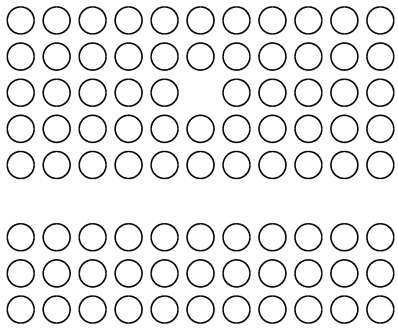

Fig. 9. Point defect and waveguide arrangement.

The complex reflection coefficients can be used to calculate the coupling of light into the defect and the overall behavior of the waveguide. Here, we choose a waveguide with a low-index core and a low-index cavity. Such structures have recently been fabricated and demonstrated to provide useful photonic crystal properties [14]. The coupling coefficient t_t is given by the transfer matrix for light crossing from the guide to the defect

$$\mathbf{M_3} = \mathbf{M_{hb}}\mathbf{M_b}\mathbf{M_{bh}} \tag{13}$$

$$t_t = \frac{2\pi}{\beta \mathbf{M_3}(2,1)}. \tag{14}$$

The coupling is usually quite small, since the light must traverse a few photonic crystal layers. As is usually done with Fabry–Perot interferometers, we compute the transmittance and reflectance of light in the waveguide through an infinite sum of light resonating in the defect. The reflectance t_b and transmittance t_f are

$$t_b = t_t^2(1 + x + x^2 + \cdots) \tag{15}$$

$$t_f = r_t - t_t^2 r_t r_x r_z e^{-i(k_z L_z + k_x L_x)}$$

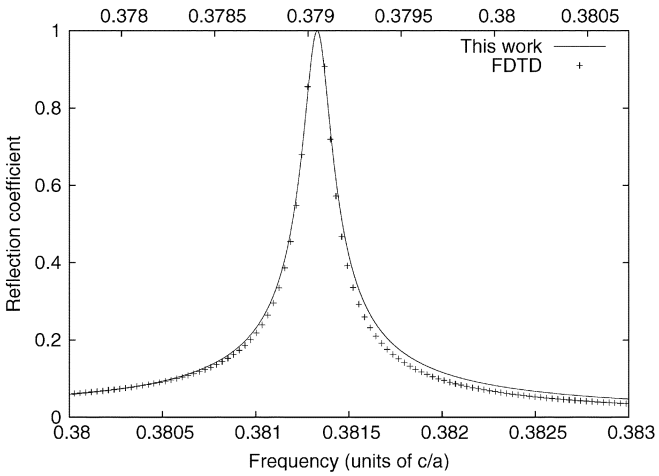

Fig. 10. Reflection and transmission in the waveguide due to defect. The lower axis is for our work, and the upper axis is for FDTD simulations.

$$\times (1 + x + x^2 + \cdots) \tag{16}$$

$$x = \left[r_x r_z e^{-i(k_z L_z + k_x L_x)} \right]^2 r_t^2 \tag{17}$$

where k_x and $k_z = \beta$ are the propagation constants in the defect, L_x and L_z are the dimensions of the defect, and r_x and r_z are the complex reflection coefficients from the defect walls; they have unit magnitude. $r_t^2 = 1 - t_t^2$ represents the fraction of the power that does not couple from the defect to the waveguide.

Fig. 10 shows the transmittance and reflectance spectra for light in the waveguide. The results have been compared with FDTD simulations. The position of the resonance agrees to within 0.8%, while its quality factor agrees within 2.4%. This disagreement is due to the numerical errors produced by FDTD when dealing with cavities with such long lifetimes. Since the quality factor is very high, we have used two horizontal axes in the figure in order to be able to show the details of the spectral features.

While in the above numerical examples we have used two-dimensional (2-D) photonic crystals for simplicity, our method is equally well suited for three-dimensional photonic crystals and for the study of 2-D photonic crystal structures etched in slab waveguides.

V. Conclusion

We have analyzed photonic crystal waveguides by separating the photonic crystal dielectric profile from the effects of the larger structure. This approach could accelerate the design of 2-D photonic crystal-based devices considerably. Moreover, the diffraction coefficients can be computed ahead of time, stored in a table, and distributed easily. The remaining steps do not require complex simulation packages. This has the potential of opening up the design of photonic crystal devices to those who do not have complex tools available, especially since our methods are close to the way we think intuitively about light in photonic crystals. Optimization of the devices is also accelerated, since the complexity of the structure is reduced considerably when introducing the effective media.

Appendix
Reflection Coefficients and Transfer Matrices

In this Appendix, we compute the boundary conditions and then set up the transfer matrices used above. We are interested in finding the Bloch modes excited in a crystal by an incoming wave, as well as the waves diffracted back into the homogeneous material. At the interface, we enforce the usual electromagnetic boundary conditions of continuity of the electric and magnetic fields. To achieve this, we decompose the Bloch modes in the plane of the interface into a 2-D Fourier series and match each Fourier component of all Bloch modes in the crystal to the corresponding diffraction order of the plane waves on the homogeneous side. When calculating the reflection and diffraction coefficients from the stopband of a crystal, the complex or nonpropagating [6], [7] Bloch modes must be used.

Working with the magnetic fields for TE polarization, the dielectric boundary conditions are

$$H_n^+ + H_n^- = \sum_j \left(H_j^{B+} B_{jn}^+ + H_j^{B-} B_{jn}^- \right) \tag{18}$$

$$\frac{1}{\epsilon_h} k_{xn} (H_n^+ - H_n^-) = \frac{1}{\epsilon_b} \sum_j \left(H_j^{B+} C_{jn}^+ + H_j^{B-} C_{jn}^- \right) \tag{19}$$

where the terms on the left-hand side of the equations denote the values in the homogeneous region, while on the right-hand side we have the photonic crystal values. H_n^+ and H_n^- represent the amplitudes of the plane waves propagating to the right, toward the interface $(+)$, and to the left, away from the interface $(-)$, with lateral propagation constant β_n. On the right-hand side, j numbers the modes, and H_j^{B+} and H_j^{B-} are Bloch modes propagating to the right and left, respectively. B_{jn} represents the nth Fourier component of mode j, corresponding to a lateral propagation vector β_n. C_{jn} represents the first derivative with respect to x of the Bloch mode Fourier components. ϵ_h and ϵ_b are the dielectric constants on the two sides of the interface. The above equations should be repeated for all diffraction orders and include all Bloch modes, both propagating and decaying, at a given frequency. In practice, however, we keep a small number of diffracted waves and Bloch modes.

Using the above equations, the reflection and diffraction coefficients are readily obtained. For example, the reflection coefficient is given by $r = H_0^-/H_0^+$. For the more complex structures in Section III, we rewrite the above equations in matrix form, to be able to use them with the TMM. For this illustration, we include only two diffraction orders. This is usually sufficient for crystals fabricated in semiconductor slab waveguides, where higher diffraction orders produce evanescent waves. The matrices are

$$\begin{bmatrix} 1 & 0 & 1 & 0 \\ 0 & 1 & 0 & 1 \\ \frac{1}{\epsilon_h} k_{x1} & 0 & -\frac{1}{\epsilon_h} k_{k1} & 0 \\ 0 & \frac{1}{\epsilon_h} k_{x2} & 0 & -\frac{1}{\epsilon_h} k_{x2} \end{bmatrix} \begin{pmatrix} H_1^+ \\ H_2^+ \\ H_1^- \\ H_2^- \end{pmatrix}$$
$$= \begin{bmatrix} B_{11} & B_{21} & B_{11} & B_{21} \\ B_{12} & B_{22} & B_{12} & B_{22} \\ \frac{1}{\epsilon_b} C_{11} & \frac{1}{\epsilon_b} C_{21} & -\frac{1}{\epsilon_b} C_{11} & -\frac{1}{\epsilon_b} C_{21} \\ \frac{1}{\epsilon_b} C_{12} & \frac{1}{\epsilon_b} C_{22} & -\frac{1}{\epsilon_b} C_{12} & -\frac{1}{\epsilon_b} C_{22} \end{bmatrix} \begin{pmatrix} H_1^{B+} \\ H_2^{B+} \\ H_1^{B-} \\ H_2^{B-} \end{pmatrix} \tag{20}$$

where we have used the following properties of the modes: $B_{jn}^{+} = B_{jn}^{-}$ and $C_{jn}^{+} = -C_{jn}^{-}$. We rewrite the above equation as

$$\mathbf{M_h V_h} = \mathbf{M_b V_b} \tag{21}$$

where the vectors $\mathbf{V_h}$ and $\mathbf{V_b}$ denote the complex field amplitudes on the homogeneous and periodic sides of the interface. We then obtain the following matrices for scattering by an interface:

$$\mathbf{V_h} = \mathbf{M_h^{-1} M_b V_b} \equiv \mathbf{M_{hb} V_b} \tag{22}$$

$$\mathbf{V_b} = \mathbf{M_b^{-1} M_h V_h} \equiv \mathbf{M_{bh} V_h}. \tag{23}$$

For propagation inside a homogeneous material or photonic crystal, the fields on the left- and right-hand sides are related by the following matrix equation:

$$\mathbf{V_l} = \begin{bmatrix} e^{ik_1 L} & 0 & 0 & 0 \\ 0 & e^{ik_2 L} & 0 & 0 \\ 0 & 0 & e^{-ik_1 L} & 0 \\ 0 & 0 & 0 & e^{-ik_2 L} \end{bmatrix} \mathbf{V_r} \tag{24}$$

where the vectors $\mathbf{V_l}$ and $\mathbf{V_r}$ represent the fields on the left and right of the region, respectively, and k_i represents the x component of the propagation vector in the homogeneous region or the possibly complex Bloch wavevector in the crystal.

REFERENCES

[1] K. S. Yee, "Numerical solution of initial boundary value problems involving Maxwell's equations in isotropic media," *IEEE Trans. Antennas Propag.*, vol. AP-14, no. 3, pp. 302–307, 1966.

[2] K. M. Leung and Y. F. Liu, "Full vector wave calculation of photonic band structures in face-centered-cubic dielectric media," *Phys. Rev. Lett.*, vol. 65, no. 21, pp. 2646–49, 1990.

[3] R. A. Shelby, D. R. Smith, and S. Schultz, "Experimental verification of a negative index of refraction," *Science*, vol. 292, no. 5514, pp. 77–79, 2001.

[4] A. Giorgio, A. G. Perri, and M. N. Armenise, "Very fast and accurate modeling of multilayer waveguiding photonic bandgap structures," *J. Lightw. Technol.*, vol. 19, no. 10, pp. 1598–1613, Oct. 2001.

[5] B. Momeni and A. Adibi, "Optimization of photonic crystal demultiplexers based on the superprism effect," *Appl. Phys. B*, vol. 77, pp. 555–560, 2003.

[6] N. Stefanou, V. Karathanos, and A. Modinos, "Scattering of electromagnetic waves by periodic structures," *J. Phys.: Condens. Matter*, vol. 4, pp. 7389–7400, 1992.

[7] T. Suzuki and K. L. Yu, "Tunneling in photonic band structures," *J. Opt. Soc. Amer. B*, vol. 12, no. 5, pp. 804–820, 1995.

[8] O. Painter, K. Srinivasan, and P. E. Barclay, "Wannier-like equation for the resonant cavity modes of locally perturbed photonic crystals," *Phys. Rev. B, Condens. Matter*, vol. 68, no. 035 214, p. 035 214, 2003.

[9] J. P. Albert, D. Cassagne, and D. Bertho, "Generalized Wannier function for photonic crystals," *Phys. Rev. B, Condens. Matter*, vol. 61, no. 7, pp. 4381–4384, 2000.

[10] S. G. Johnson and J. D. Joannopoulos, "Block-iterative frequency-domain methods for Maxwell's equations in a planewave basis," *Opt. Express*, vol. 8, no. 3, pp. 173–190, 2001.

[11] S. Boscolo, M. Midrio, and C. G. Someda, "Coupling and decoupling of electromagnetic waves in parallel 2-D photonic crystal waveguides," *IEEE J. Quantum Electron.*, vol. 38, no. 1, pp. 47–53, Jan. 2002.

[12] P. Yeh, *Optical Waves in Periodic Media*. New York: Wiley, 1988.

[13] Y. Akahane, M. Mochizuki, T. Asano, Y. Tanaka, and S. Noda, "Design of a channel drop filter by using a donor-type cavity with high-quality factor in a two-dimensional photonic crystal slab," *Appl. Phys. Lett.*, vol. 82, no. 9, pp. 1341–1343, 2003.

[14] M. Tokushima, H. Yamada, and Y. Arakawa, "1.5 μm wavelength light guiding in waveguides in square-lattice-of-rod photonic crystal slab," *Appl. Phys. Lett.*, vol. 84, no. 21, pp. 4298–4300, 2004.

Emanuel Istrate (S'96) received the Bachelor's of Applied Science degree in engineering science from the University of Toronto, Toronto, ON, Canada, where he is currently working toward the Ph.D. degree.

His research interests include photonic crystals and passive optic devices.

Edward H. Sargent (M'97–SM'98) received the B.Sc.Eng. degree in engineering physics from Queen's University, Kingston, ON, Canada, in 1995 and the Ph.D. degree in electrical and computer engineering (photonics) from the University of Toronto, Toronto, ON, Canada, in 1998.

He is the 2004–2005 Visiting Professor in nanotechnology and photonics with the Massachusetts Institute of Technology (MIT) Microphotonics Laboratory, Cambridge. He holds the Nortel Networks—Canada Research Chair in Emerging Technologies with the Department of Electrical and Computer Engineering, University of Toronto.

Prof. Sargent was named "one of the world's top young innovators" by MIT's *Technology Review* magazine in 2003. In 2002, he was celebrated by the IEEE "for groundbreaking research in applying new phenomena and materials from nanotechnology toward transforming fiber-optic communications systems into agile optical networks."